

Disinfection of *S. mutans* Bacteria Using a Plasma Needle at Atmospheric Pressure

J. Goree, *Member, IEEE*, Bin Liu, David Drake, and E. Stoffels

xxx

Abstract— *Streptococcus mutans* (*S. mutans*) bacteria were killed using a low-power millimeter-size atmospheric-pressure glow discharge plasma, or plasma needle. The plasma was applied to a culture of *S. mutans* that was plated onto the surface of an agar nutrient in a Petri dish. *S. mutans* is the most important microorganism for causing dental caries. Images of the sample, taken after both plasma treatment and incubation, reveal that *S. mutans* was killed with a spatial pattern that varied depending on the plasma operating parameters. Bacteria were killed in either a solid circle as would be desirable for dental treatment, or in an undesirable ring. The ring-shaped pattern is explained by the shape of the glow, as revealed by Abel-inverted images. Temperature measurements in the agar verify that the observed killing was not due to heat. The presence of the radicals OH and O was verified using optical emission spectroscopy.

Index Terms—Microorganisms, Sterilization, Plasma applications, Non-thermal plasma, Micro-plasma, Atmospheric glow discharge

I. INTRODUCTION

ATMOSPHERIC glow discharges show considerable promise for decontamination applications, where surfaces are exposed to plasma in order to destroy microorganisms. Of interest here are non-thermal glow discharges, i.e., non-equilibrium plasmas with gas at nearly the same temperature as the ambient gas, in contrast to thermal plasmas or arcs [1-7]. For biomedical applications, atmospheric conditions are essential because samples cannot be inserted into a vacuum chamber.

Atmospheric glow discharges produce short-lived chemical species, which are propelled by the low-temperature gas toward a surface that is to be treated. The short life of these species is desirable because they do not remain after the treatment is completed.

With appropriately designed electrodes, power supply and gas supply, an atmospheric glow discharge can be operated stably, below the glow-to-arc transition. This generally requires

one or more of the following design features: using inert gas such as helium to lower the breakdown voltage, a significant gas flow rate, high-frequency power, a cathode with sharp features to increase the local electric field, and a dielectric barrier on the electrodes. The device studied here has most of these features.

Our “plasma needle” device produces a small-diameter low-power atmospheric-pressure glow discharge. It is intended for dental or medical applications [8-15]. Radio-frequency high voltage is applied to a single needle electrode located inside a concentric gas-flow nozzle. The nozzle has a diameter of a few millimeters, and the plasma that flows out of the nozzle has a comparable diameter. This design is similar to the so-called microbeam plasma generator [7]. The nozzle is placed a few millimeters from the surface that is to be treated, and the plasma jet is directed onto that surface. When desired, the plasma needle can be operated at a power so low that the glow is barely visible to the unaided eye.

Using small-diameter plasma allows site-specific disinfection of spots with a diameter of a few millimeters. This small size distinguishes the plasma needle from larger atmospheric-glow devices intended to sterilize large-area contaminated surfaces [16-20]. For dental or medical use, a disinfection method should be precise enough to treat small areas, and it should operate at a low power to avoid damaging healthy tissue by heating.

One proposed application for the plasma needle is the treatment of dental caries [11]. The most significant cariogenic microorganism is *Streptococcus mutans* (*S. mutans*). This is a gram-positive, facultatively anaerobic microorganism that forms biofilms on teeth (dental plaque), penetrates into fissures, and erodes the enamel and dentine. In clinical practice, caries are treated by drilling, which removes healthy tissue along with the infected dentine. It would be desirable to ensure disinfection before placement of restorative materials by destroying the bacteria in a cavity without harming healthy tissue. Unfortunately, current chemotherapeutic agents, such as chlorhexidine, have undesirable side effects, including disagreeable taste and stains [21]. Plasma needle treatment is unlikely to have these disadvantages, and it offers some promise for painless treatment as well.

The most important bacterium for causing caries is *Streptococcus mutans*, or *S. mutans*. Since it is a facultative anaerobe, it can grow in the presence of oxygen as it does in the mouth, but it prefers oxygen-poor conditions. It penetrates into

Manuscript received October 9, 2005.

J. Goree and Bin Liu are with the Department of Physics and Astronomy, The University of Iowa, Iowa City, IA 52242 USA (phone 319-335-1843; fax: 319-335-1753)

David Drake is with the Dows Institute for Dental Research, Dept. of Endodontics, College of Dentistry, The University of Iowa, Iowa City, IA 52242 USA

E. Stoffels is with the Faculty of Biomedical Engineering, Eindhoven University of Technology, Eindhoven, The Netherlands.

fissures where it is well-protected from oxygen and from the natural antimicrobial activity of saliva. Its temperature range for growth is 30° C to 47° C, with optimal growth at human body temperature, 37° C. Heat kills *S. mutans* at temperatures above 60° C [22].

Individual *S. mutans* bacteria are relatively easy to kill. However, they form thick biofilms in the presence of sucrose consisting of high molecular weight glucans. This layer is rather difficult to penetrate. Antibacterial treatment methods that have been used for *S. mutans* include rinsing with chemical solutions such as chlorhexidine [21, 23] and laser irradiation [24].

For clinical use in dentistry, it is important to distinguish whether any observed bactericidal effect is due to chemical species or heat. The heating of teeth should be avoided because a tooth suffers pulpal necrosis in 15% of cases when heated by more than 5.5° C, and in 60% of cases when heated by more than 11° C [25].

What makes the plasma needle appealing is that it produces short-lived chemical species in the gas phase. These can impinge on a tooth's surface, and they can dissolve into a liquid [15]. Unlike liquid rinses with bactericidal ingredients that linger in the mouth after treatment, the plasma needle produces bactericidal agents locally. Once the treatment is completed, no excess radicals remain, due to recombination among themselves or by reacting with ambient air and water molecules. Thus, the bactericidal agents have a naturally short lifetime, which is an attractive feature.

At the present time, it is not known exactly which species produced by a plasma needle applies the greatest bactericidal effect, or where it is formed. Radical formation can occur either in the gas phase or in a liquid. In both cases, the process begins with energetic electrons in the plasma. In the gas phase, atomic oxygen O and hydroxyl OH radicals are produced by electron-impact dissociation of air molecules H₂O and O₂ [12, 15]. These two radicals, O and OH, are both known to have a bactericidal effect [26, 27]. Radical formation in the liquid phase is a more complicated process, beginning with helium atoms in the gas phase that are excited to a metastable state due to electron impact. These metastable atoms subsequently enter the aqueous sample, where they produce radicals *in situ* by dissociating H₂O.

In this paper we demonstrate that the plasma needle is capable of treatment under conditions that are attractive to dentistry. It can kill *S. mutans* with a treatment time of tens of seconds, and without heating a sample significantly. We found that the killing is reproducible for the conditions that are most attractive for clinical use. The shape of the spot where *S. mutans* are killed depends on the plasma operating parameters: it is either a desirable homogeneous circle, or an undesirable ring when the glow is similarly ring-shaped.

II. PROCEDURE

A. Sample preparation

Bacteria culture was plated on agar plates, forming a bacterial lawn. Plastic Petri dishes were filled to a depth of 4 mm with agar, which is an aqueous growth medium with a jelly-like consistency. After cooling and solidification, dishes were inoculated with *S. mutans* using a spiral-plating technique. This was done in a Spiral Biotech Autoplate 4000, which resembles a phonograph record player, with a turntable that rotates the dish while a dispensing stylus applies the bacterial solution. The bacterial concentration was 10⁶-10⁷ colony-forming units per milliliter suspension. The resulting spiral-shaped line formed a bacterial lawn covering the surface of the agar. The 12-mm diameter center of the dish was not inoculated.

Similar dishes, but without bacteria, were prepared for temperature tests. These dishes were filled with agar to the same 4 mm depth, but we immersed temperature-sensitive indicator strips halfway deep in the agar. These strips have a pattern of white dots to indicate the temperature. If the temperature exceeds the indicated value for a dot, it irreversibly turns black; otherwise it remains white. In this way, we were able to measure the temperature increase of our sample during treatment. A limitation of this scheme is that we measured the temperature 2 mm below the agar surface, not on the surface where the bacteria were located.

Spiral-plating yields a sample with bacteria localized on a surface, and not dispersed in a volume. This is suitable for testing the plasma needle, because plasma treatment is essentially a surface treatment. However, plasma-generated radicals can be absorbed into the volume of a water sample, with a penetration depth of several mm [15].

Before using the spiral-plating method, we attempted with less success to perform sterilization tests with bacteria suspended in the volume of a 100 μL water droplet resting on a Petri dish. After treatment, the suspension was collected with a pipette and then cultured. This scheme has the advantage of allowing a convenient census of bacterial colonies, but it is better suited for bactericidal treatments that act in a volume rather than on a surface. We found that the small droplet was greatly diminished by evaporation during plasma treatment. This method also did not allow imaging the treatment spots, as we did here.

B. Plasma needle apparatus

We used a plasma needle similar to the design reported in [11]. It consists of a handset, a gas supply, and a high-frequency generator. The handset, Fig. 1(a), has three fittings: a gas inlet, an electrical feedthrough, and a nozzle. The most important features are inside the nozzle, Fig. 1(b). At the center of the nozzle is a tungsten neurology needle, with a diameter of 0.2 mm and a pencil-shaped taper of length 0.6 mm. The tip was sharp, but it dulled after operating the plasma over time, as indicated by a slight increase in breakdown voltage.

The needle was concentric with a cylindrical glass tube nozzle, with an inside diameter $D = 4$ mm and an outside diameter of 6.35 mm. The needle shaft was covered with a ceramic insulator tube, leaving a length $L = 5.7$ mm of the needle exposed to gas. Along this length, and at the tip itself, a glow can form. The nozzle was flush with the needle tip.

We used pure helium, which was found in earlier tests to offer a lower breakdown voltage and more stability from the glow-to-arc transition, as compared to other gas mixtures [11]. It is unattractive to add gases such as O_2 directly into the gas feed because, contrary to what one might expect, this diminishes the production of radicals, presumably due to electron attachment inside the nozzle [15]. For producing radicals in the gas phase, we rely on mixing air into the flow downstream of the nozzle.

The needle electrode was powered by 7.17 MHz radio-frequency high voltage. To provide a return current, a grounded metal plate was positioned below the plastic Petri dish, as shown in the scale drawing of Fig. 1(b) and the sketch of Fig. 1(c). However, the discharge can be maintained even without the grounded metal plate, as might be the case for clinical applications.

Clinical applications would require a compact portable generator, which should couple radio-frequency power efficiently to the plasma so that excessive voltages are not required to achieve breakdown. The generator setup we used, however, was bulky and the network was unable to match efficiently to the high impedance of the plasma. Most of the radio-frequency power was deposited into cables or elsewhere in the network, and not in the plasma. Moreover, our needle and nozzle design is probably not optimal. As a result, attaining gas breakdown required a higher voltage of typically 600 V peak-to-peak, as compared to 200 V for another plasma needle setup [11].

Our network consisted of a tee-configuration matchbox intended for amateur radio, followed by an autotransformer coil to boost the output impedance, as sketched in Fig. 1(c). The peak-to-peak voltage was measured with a digital-storage oscilloscope using a Tektronix P5100 high-voltage probe that contacted the rf conductor. The probe location was 80 mm from the needle tip; therefore, the voltage measured does not necessarily indicate the voltage on the tip itself. Thus, there are two reasons our voltage measurements are useful only for relative comparisons, and not for comparison to other setups: our network did not match the plasma impedance, and our probe did not necessarily measure the voltage at the needle's tip.

The gas flow from the nozzle is important for several reasons. First, it is helpful in achieving breakdown. Second, the flow mixes downstream from the nozzle with atmospheric gases including N_2 , O_2 and H_2O . Third, the gas flow propels radicals and metastables toward the surface to be treated. Fourth, the flow diameter helps determine the diameter of the treated spot on the sample. The flow rate was an adjustable parameter, and it was measured using a Sierra mass flow meter. The flow velocity V in the glass-tube nozzle is proportional to

the flow rate; at a flow rate of 1 SLPM (liters per minute), the velocity is $V = 1.3$ m/s. This gas flow is comfortable in the mouth.

We positioned the handset using a mechanical setup with the needle pointed downward toward the sample. The sample's agar surface was horizontal, so that the gas flow impinged the sample's surface at a 90° incidence. The handset was held in a mount that allowed raising and lowering it.

C. Optical diagnostics for the glow

We tested for the presence of radicals using optical-emission spectroscopy (OES). At one end of an optical fiber, light was coupled into the entrance slit of a Ocean Optics HR2000 spectrometer, with a 300 lines/mm grating. The other end of the fiber collected light focused by a pair of fused silica convex lenses, Fig. 1(c). To detect only light produced downstream from the nozzle, we positioned a razor blade in the focal plane between the lenses to block light produced inside the glass tube.

We also imaged the glow. This was done under the same operating conditions as for bactericidal treatment, but with the plasma impinging on a clean 5-mm thick glass plate substituted for the Petri dish with agar. The Dalsa 1M30 camera that was used has a 12-bit monochrome CCD with a linear response so that the pixel values recorded are proportional to the actual light intensity. The exposure time was 1/30 sec; longer exposures are impractical because small atmospheric winds deflect the glow. Using a 105-mm focal-length Nikon micro lens with no spectral filter, we imaged all wavelengths in the visible and near IR, which consisted mostly of He spectral lines. When viewing these images, it is useful to remember that brightness in the image reveals only the presence of energetic electrons, and not necessarily the presence of bactericidal agents. Energetic electrons can only produce radicals if air is mixed into the flow.

To reveal the true spatial profile of the emission, we transformed the images using Abel inversion. The observed image $i(x, z)$ is a projection of the emission onto an xz plane, where z is the height above the sample surface. To compute the emission function $I(r, z)$, we used the reverse Abel transform,

$$I(r, z) = -\frac{1}{\pi} \int_r^\infty \frac{di(x, z)}{dx} \frac{dx}{\sqrt{x^2 - r^2}}, \quad (1)$$

which assumes a circularly symmetric plasma.

D. Plasma treatment

There were four adjustable parameters for our plasma treatment. The exposure time was varied in a range from 10 to 120 sec, the needle-to-sample separation d from 2 to 4 mm, the RF peak-to-peak voltage from 600 to 900 V, and the gas flow from 0.2 to 4.0 SLPM.

To begin, we raised the handset, installed a Petri dish with its center immediately below the needle, and then lowered the handset to the desired separation d . At this time the plasma

impinged on the center of the dish, which was not inoculated.

Next, we began plasma treatment by positioning the Petri dish so that the plasma impinged on a desired spot in the inoculated portion of the dish. At the end of the exposure time, we moved the dish to treat another spot. We repeated this step to treat a total of five spots on the dish, as shown in Fig. 2.

Finally, as the control for the experiment, we moved the Petri dish to treat a sixth spot, and simultaneously we switched the plasma off while allowing the gas to continue flowing. As a control, this spot indicates the effects of helium flow without any plasma-generated species.

During plasma treatment, we observed that the surface of the agar gradually became indented, especially when operating at high voltages, small separations, and long exposures. This depression was presumably due to evaporation. Based on our imaging results, presented later, we assume that only aqueous components of the agar evaporated, while the bacteria on the remained on the surface.

E. Avoiding the glow-to-arc transition

Sometimes the glow underwent a transition to a filamentary arc. When this happened, the plasma had a more concentrated shape and there was an audible hissing noise. We found that a reliable visual indication of nearing the glow-to-arc transition was the length l of the glow along the needle shaft. In a stable glow discharge operation, the glow was concentrated only at the tip, $l \ll L$. However, as the voltage was increased or the separation d was decreased, l gradually increased and audible hiss became more noticeable; we refer to these conditions slightly below the glow-to-arc transition as “hot.” It is possible that a filament was present within the glow under hot conditions, although we have no evidence of this. Finally, the entire glow transitioned to a filamentary arc when the glow touched the insulator, $l = L$. When this happened, the sample burned where it was touched by the arc, and we discontinued treatment.

For clinical practice, it would be necessary to suppress arcs. The authors believe that improvements in generator design and nozzle design will make this possible. Otherwise, arcs could occur when the practitioner positions the handset too near the surface to be treated.

F. Incubation and imaging

To visually observe the effect of plasma treatment, the treated samples were incubated so that visible colonies formed. This was done using the following procedure. After treatment with the plasma needle, the Petri dishes were covered to prevent atmospheric contamination. At this time, the treated spots were not yet identifiable by any color change in the sample. The dishes were then installed in a CO₂ incubator at 37° C for 48 hours so that bacteria multiplied and formed colonies. After incubation we imaged the dishes with a digital color camera using white photographer’s lights for illumination.

The lawn of bacterial colonies changed color and became visible to the naked eye after incubation, as seen in Fig. 2. Color

is our primary indicator of bactericidal effect. Light brown indicates living colonies, whereas dark brown indicates an absence of living colonies. The purpose of the images is to reveal qualitatively whether bacteria were killed, and where. We did not attempt to quantify the killing, for example in terms of the fraction of bacterial colony-forming units that survived treatment.

G. Temperature tests

After applying plasma treatment to the dishes that were inoculated with bacteria, we then applied a similar treatment to the dishes with temperature-sensitive strips rather than bacteria. We varied the same four parameters as in the tests with the bacterial samples.

III. RESULTS

A. Optical emission spectra results

The optical emission spectrum verifies the presence of O and OH radicals. This is shown in Fig. 3 and Table I. Similar spectra for a plasma needle device were reported previously [11]. The radicals O and OH are known to be bactericidal.

B. Temperature test results

In our temperature tests, we sought to determine the conditions where the agar temperature increased above 40 °C. For comparison, *S. mutans* grows at temperatures up to 47 °C, and it is killed by heat at temperatures above 60 °C [22].

Under most conditions, the agar temperature remained below 40 °C. From this result we conclude that it is possible to operate a plasma needle so that there is no killing due to heat.

TABLE I
FOR THE SPECTRAL LINES OBSERVED IN FIG. 3, STANDARD
WAVELENGTHS ARE LISTED HERE [28, 29]

Species	Wavelength (nm)	Species	Wavelength (nm)
O	777.19	N ₂ ⁺	391.44
	844.64		427.81
			470.92
OH	306.4 system:		
	306.36		
	306.72		
	307.8		
	308.9		
He	492.19	N ₂	315.93
	501.57		337.13
	587.56		353.67
	656.01		357.69
	667.82		375.54
	706.52		380.49
	728.14		

Heating above 40 °C was observed only for extreme conditions. For example, the agar temperature did not exceed 40 °C for the conditions of $V_{pp} = 800$ V, $d = 3$ mm, 1.5 SLPM, and an exposure time of 30 s, which we classify as “warm” conditions based on the shape of the treatment spot, shown later. However, the agar temperature did exceed 40 °C when we either decreased the separation to 2.5 mm, increased the voltage to 900 V, or increased the exposure time to 60 sec. For clinical applications, these conditions would also be unattractive for other reasons. As we will see in the images of the Petri dishes, operating with small separation d , large voltage, and large gas flow leads to an undesirable shape for the treatment spot. A long exposure time > 60 sec would be impractical for clinical use in dentistry.

C. Bacteriology results

The killing of *S. mutans* by plasma treatment is shown by the dark treatment spots in the Petri dishes, after incubation. In Fig. 2, spots 1-5 were treated identically, and their darkness indicates a bactericidal effect. This effect shows consistent reproducibility in all five treated spots.

Control spot 6, on the other hand, appears the same as its surroundings. This control spot was treated with the handset positioned at the same distance d , the same gas flow, and the same duration as for spots 1-5, but the high voltage that sustains the plasma was turned off.

Comparing spots 1-5 with the control spot 6 allows us to conclude that the bactericidal effect is due to the plasma. However, it remains unknown which plasma-generated species is dominant. As discussed in Section I, candidates include O and OH radicals produced by electron-impact dissociation in the gas, or possibly metastable He produced in the gas that subsequently enters the aqueous sample and produces radicals *in situ* by dissociating H₂O.

The shape of the treatment spot varied, depending on the operating conditions. The results that are most encouraging for possible clinical use are shown in Fig. 2. The spatial pattern in this case was a circular spot, indicating a killing effect that was spatially homogenous within a diameter of 5 mm. Conditions leading to a homogenous circle are, in general, low voltage, low flow rate, large separation d , and a moderately short exposure time. We refer to these conditions as “cool.” For Fig. 2, the parameters were $V_{pp} = 600$ V, 1.5 SLPM, $d = 3$ mm, and exposure time 30 s.

The shape of the treatment spot changed from a homogenous circle to a ring as conditions were changed from cool to warm. This happens when the voltage, flow and exposure time were increased, and as the separation was decreased. In Fig. 4, each row corresponds to changing a single parameter such as V_{pp} while holding other parameters constant. The results are also organized in columns, so that similarly shaped spots can easily be compared.

We next consider the effects of varying each parameter individually.

As the voltage is increased in Fig. 4(b), we see that beginning with the same homogenous spot as in Fig. 2 at low voltage, the spot shape changes to a ring in the second column. There was

no significant killing inside the ring. As the voltage is increased further, a central spot appears inside the ring; this occurs for parameters we term “hot,” which are typically near the glow-to-arc transition. We speculate that the central spot is due to killing bacteria with heat, perhaps by a filament in the glow, but we have no direct evidence of this.

As the exposure time is increased in Fig. 4(a), killing increases as indicated by the expansion of the dark area in the ring, and the central spot begins to develop.

As the flow rate is increased in Fig. 4(c), the desirable homogenous circle becomes a ring with a central spot. Further increases in the flow rate, however, do not continue this trend, as we will report in a separate paper.

As the separation is decreased, the same trend occurs as when any of the other three parameters are increased. In Fig. 4(d) the homogeneous circle becomes a ring. At higher voltages in Fig. 4(e) when the separation is decreased the ring can develop a central spot.

We note that evaporation during treatment apparently did not remove bacteria from the sample. As we discussed earlier, the agar surface became indented during treatment, apparently due to evaporation. This depression was deepest in the center of a spot. However, the center of the spots did not seem to lose any bacteria, as can be seen in the ring-shaped spots for the warm conditions.

To summarize, there are three general shapes we observed in the killing pattern: a homogeneous circle for cool conditions, a ring for warm conditions, and a ring with a central spot for hot conditions. Cool conditions are most attractive for possible clinical applications, and these are achieved at low values for voltage and exposure time but large separation.

D. Images of the glow

Recall that the glow is produced by electron-impact excitation of gas atoms, so that it serves as a visual indicator of the presence of energetic electrons. These energetic electrons are also capable of generating radicals, either directly by dissociating gas molecules such as H₂O and O₂, or indirectly by generating metastable He atoms that might possibly enter a liquid and dissociate H₂O molecules *in situ*. The light emission is not an indicator of the radicals themselves, but merely an indicator of one of the components required to produce them. To produce OH or O radicals in the gas phase requires that H₂O and O₂ be mixed into the glow so that energetic electrons can dissociate them.

Side-view images are shown in Fig. 5. The left column shows the image as recorded by the camera, while the right column shows the Abel-inverted images. The latter are more instructive. For cool conditions, as in the top row of Fig. 5, the glow is concentrated in a narrow column of diameter 3 mm. For hot conditions, as in the bottom row of Fig. 5, the glow spreads out to a larger diameter, and it develops into a ring just above the sample surface.

The shape of the glow helps explain the shape of the treatment spots. This is demonstrated in Fig. 6, where the Abel-inverted image of the glow is aligned with a

corresponding image of the sample. For cool conditions in the left column, a glow shaped like a narrow column yields a treatment spot that is a homogeneous circle. For hot conditions in the right column, a glow that is ring-shaped near the sample yields a treatment spot that has a similar ring shape.

IV. CONCLUSION

We demonstrated that the plasma needle is capable of treatment under conditions that are attractive to dentistry. We demonstrated that it is capable of killing *S. mutans*. It can kill with a treatment time of tens of seconds, and without an elevated temperature. We found that the plasma needle can be operated under conditions where the bactericidal effect is attributable to atmospheric chemical species produced by the plasma and not due to heat. We also found that the spot where *S. mutans* are killed can be shaped into a desirable homogeneous circle by choosing cool operating conditions. The shape of this spot is reproducible for cool conditions. We also identified some issues that require further work before the device can be used clinically.

ACKNOWLEDGMENT

We thank S. Clark, V. Nosenko, F. Skiff, R. Vogel and J. Wefel for useful discussions.

REFERENCES

- [1] S. Kanazawa, M. Kogoma, T. Moriwaki, and S. Okazaki, "Stable glow plasma at atmospheric pressure," *J. Phys. D*, Vol. 21, pp. 838-840, 1988.
- [2] S. Okazaki, M. Kogoma, M. Uehara, and Y. Kimura, "Appearance of stable glow discharge in air, argon, oxygen and nitrogen at atmospheric pressure using 50 Hz source," *J. Phys. D*, Vol. 26, pp. 889-892, 1993.
- [3] A. Schütze, J. Y. Jeong, S. E. Babayan, J. Park, G. S. Selwyn, and R. F. Hicks, "The atmospheric-pressure plasma jet: a review and comparison to other plasma sources," *IEEE Trans. Plasma Sci.*, Vol. 26, pp. 1685-1694, 1998.
- [4] J. Park, I. Henins, H. W. Hermann, and G. S. Selwyn, "An atmospheric-pressure plasma source," *Appl. Phys. Lett.*, Vol. 76, pp. 288-290, 2000.
- [5] J. Park, I. Henins, H. W. Hermann, and G. S. Selwyn, "Discharge phenomena of an atmospheric pressure radio-frequency capacitive plasma source," *J. Appl. Phys.*, Vol. 89, pp. 20-28, 2001.
- [6] M. M. Kzkez, M. R., Barrault, and J. D. Craggs, "Spark channel formation," *J. Phys. D*, Vol. 3, pp. 1886-1896, 1970.
- [7] H. Koinuma, H. Ohkubo, and T. Hashimoto, "Development and application of a microbeam plasma generator," *Appl. Phys. Lett.*, Vol. 60, pp. 816-817, 1992.
- [8] E. Stoffels, A. J. Flikweert, W. W. Stoffels, and G. M. W. Kroesen, "Plasma needle: a non-destructive atmospheric plasma source for fine surface treatment of (bio)materials," *Plasma Sources Sci. Tech.*, Vol. 11, pp. 383-388, 2002.
- [9] E. Stoffels, I. E. Kieft, and R. E. J. Sladek, "Superficial treatment of mammalian cells using plasma needle," *J. Phys. D*, Vol. 23, pp. 2908-2913, 2003.
- [10] E. A. Sosnin, E. Stoffels, M. V. Erofeev, I. E. Kieft, and S. E. Kunts, "The effects of UV irradiation and gas plasma treatment on living mammalian cells and bacteria: A comparative approach," *IEEE Trans. Plasma Sci.*, Vol. 32, pp. 1544-1550, 2004.
- [11] R. E. J. Sladek, E. Stoffels, R. Walraven, P. J. A. Tielbeek, and R. A. Koolhoven, "Plasma treatment of dental cavities: A feasibility study," *IEEE Trans. Plasma Sci.*, Vol. 32, pp. 1540-1543, 2004.
- [12] I. E. Kieft, E. P. van der Laan, and E. Stoffels, "Electrical and optical characterization of the plasma needle," *New Journal of Physics*, Vol. 6, p. 149, 2004.
- [13] I. E. Kieft, D. Darios, A. J. M. Roks, and E. Stoffels, "Plasma treatment of mammalian vascular cells: A quantitative description," *IEEE Trans. Plasma Sci.*, Vol. 33, pp. 771-775, 2005.
- [14] R. E. J. Sladek and E. Stoffels, "Deactivation of *Escherichia coli* by the plasma needle," *J. Phys. D*, Vol. 38, pp. 1716-1721, 2005.
- [15] I. E. Kieft, J. J. B. N. Van Berkel, E. R. Kieft, and E. Stoffels, "Radicals of plasma needle detected with fluorescent probe," in *Plasma Processes & Polymers, Plasma Processes and Polymers*, Riccardo d'Agostino, Pietro Favia, Christian Oehr, and Michael R. Wertheimer Ed., Weinheim Germany: Wiley VCH, 2005, pp.295-308.
- [16] M. Laroussi, "Sterilization of contaminated matter with an atmospheric pressure plasma," *IEEE Trans. Plasma Sci.*, Vol. 24, pp. 1188-1191, 1996.
- [17] H. W. Hermann, I. Henins, J. Park and G. S. Selwyn, "Decontamination of chemical and biological warfare (CBW) agents using an atmospheric pressure plasma jet (APPJ)," *Phys. Plasmas*, Vol. 6, pp. 2284-2289, 1999.
- [18] T. C. Montie, K. Kelly-Wintenberg, and J. R. Roth, "An Overview of research using the one atmosphere uniform glow discharge plasma (OAUGDP) for sterilization of surfaces and materials," *IEEE Trans. Plasma Sci.*, Vol. 28, pp. 41-50, 2000.
- [19] M. Laroussi, "Nonthermal decontamination of biological media by atmospheric-pressure plasmas: review, analysis, and prospects," *IEEE Trans. Plasma Sci.*, Vol. 30, pp. 1409-1415, 2002.
- [20] M. Vleugels, G. Shama, X., T. Deng, E. Greenacre, T. Brocklehurst, and M., G. Kong, "Atmospheric plasma inactivation of biofilm-forming bacteria for food safety control," *IEEE Trans. Plasma Sci.*, Vol. 33, pp. 824 - 828, 2005.
- [21] E. A. Kidd, "Role of chlorhexidine in the management of dental caries," *International Dent J.*, Vol. 41, pp.279-286, 1991.
- [22] Y. Ma, R. E. Marquis, "Thermophysiology of *Streptococcus mutans* and related lactic-acid bacteria," *Antonie Van Leeuwenhoek*, Vol. 72, pp. 91-100, 1997.
- [23] A. J. McBain, R. G. Bartolo, C. E. Catrenich, D. Charbonneau, R. G. Ledder, P. Gilbert, "Effects of chlorhexidine gluconate-containing mouthwash on the vitality and antimicrobial susceptibility of in vitro oral bacterial ecosystems," *Appl. Environm. Microbiol.*, Vol. 69, pp. 4770-4776, 2003.
- [24] I. Ishikawa, J. Frame, A. Aoki, editors, "Lasers in dentistry: revolution of dental treatment in the new millennium," *International Congress series 1248*, Elsevier, 2003.
- [25] L. Zach and G. Cohen, "Pulp response to externally applied heat," *Oral Surgery, Oral Medicine, Oral Pathology*, Vol. 19, pp. 515-530, 1965.
- [26] J. Verhoef, "The phagocytic process and the role of complement in host defense," *J. Chemother. Suppl.*, Vol. 1, pp. 93-97, 1991.
- [27] J. M. Gutteridge, G. J. Quinlan, P. Kovacic, "Phagomimetic action of antimicrobial agents," *Free Radic. Res*, Vol. 28, pp. 1-14, 1998.
- [28] A. N. Zaidel', V. K. Prokof'ev, S. M. Raiskii, V. A. Slavnyi, and E. Ya. Shreider, *Tables of Spectral Lines*, New York: IFI/Plenum Data Corporation, 1970.
- [29] R. W. B. Pearse and A. G. Gaydon, *The Identification of Molecular Spectra*, 3rd ed., New York: John Wiley & Sons Inc., 1963.

FIGURE CAPTIONS

1. Plasma needle setup. (a) The handset was a nylon Swagelok tee, with the nozzle pointed downward. (b) This scale drawing of the nozzle includes a sketch showing where the glow was visible. Bacteria were plated on the surface of the agar. (c) RF network and optical glow diagnostics, not drawn to scale.
2. Petri dish, imaged after treatment and incubation. A light color indicates living bacteria colonies. The spiral pattern is due to the inoculation method; the center was never inoculated. Plasma treatment, applied to spots 1-5, killed the *S. mutans* bacteria, as indicated by the dark color. Spot 6 was a control, with treated with gas flow but no plasma; it appears the same as the surrounding untreated areas. Treatment conditions were 1.5 SLPM, $d = 3$ mm, $V_{pp} = 600$ V, and exposure time 30 s.
3. Spectrum of the optical emission from the glow, downstream of the nozzle, for the same conditions as Fig. 2. Note the lines for OH and O, which are bactericidal agents produced by the plasma. Wavelengths are listed in Table I.
4. Treatment spots imaged after treatment and incubation, for various plasma treatment parameters. In each row, one parameter was adjusted. Columns are aligned to show similar killing patterns: a desirable spot in the left column, a ring in the second column, and a ring with a central spot in the two columns to the right. The latter two columns correspond to “hot” conditions near the glow-to-arc transition. (a) V_{pp} was increased. (b) Exposure time was increased. (c) Flow rate was increased. (d-e) the separation d was decreased. Except where indicated otherwise, parameters were 1.5 SLPM, $d = 3$ mm, $V_{pp} = 800$ V, and exposure time 30 s.
5. Images of the glow as viewed from the side. The sample surface at the bottom, $z = 0$, was a glass plate substituted for the agar and Petri dish. The nozzle end at $z = 3$ mm is not visible in these images. The left column shows images as recorded by the camera, while the right column shows the corresponding images after Abel inversion, using (1), to reveal the radial distribution of the intensity. Parameters were 1.5 SLPM and $d = 3$ mm.
6. Abel-inverted images (top) and images of spots on Petri dishes (bottom), at the same scale. For cool conditions (left column), the glow was a narrow column, yielding a killing pattern with a homogeneous circle of diameter 5 mm. For hot conditions (right column), the ring, with its 5-mm inside diameter, corresponds to a bright ring in the glow at $(r,z) = (2.5$ mm, 0.5 mm). Comparing these images of the glow and the Petri dish helps explain the shape of the treatment spot. Parameters were 1.5 SLPM, $d = 3$ mm, and 30 sec exposure.

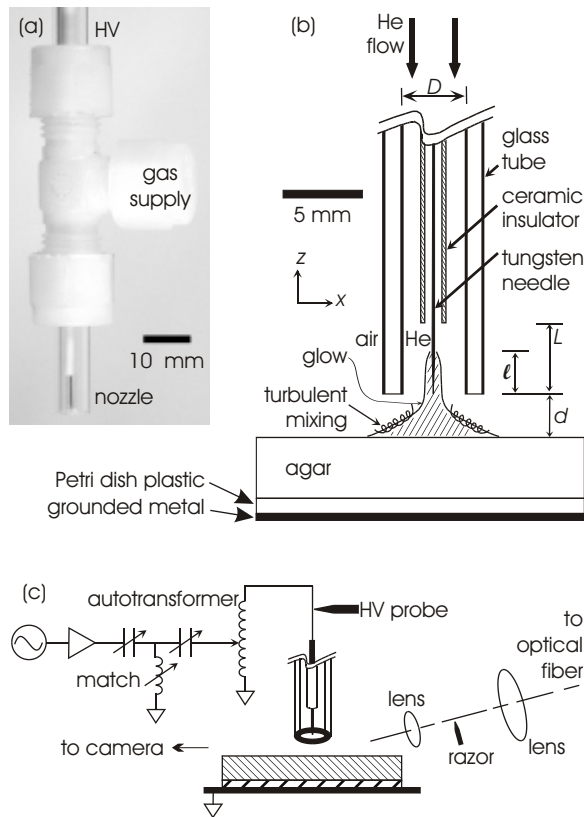


Fig.1

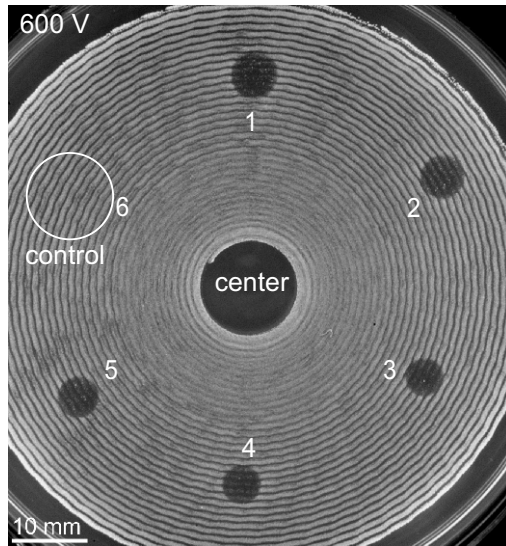


Fig. 2

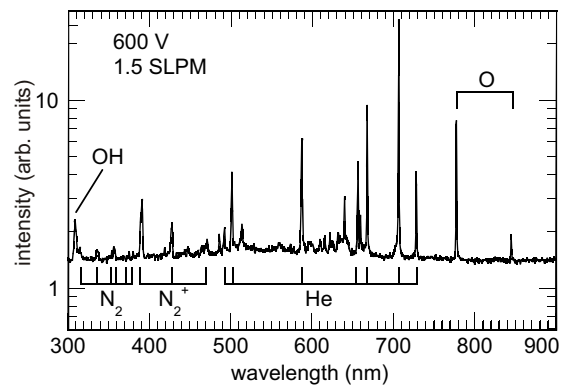


Fig. 3

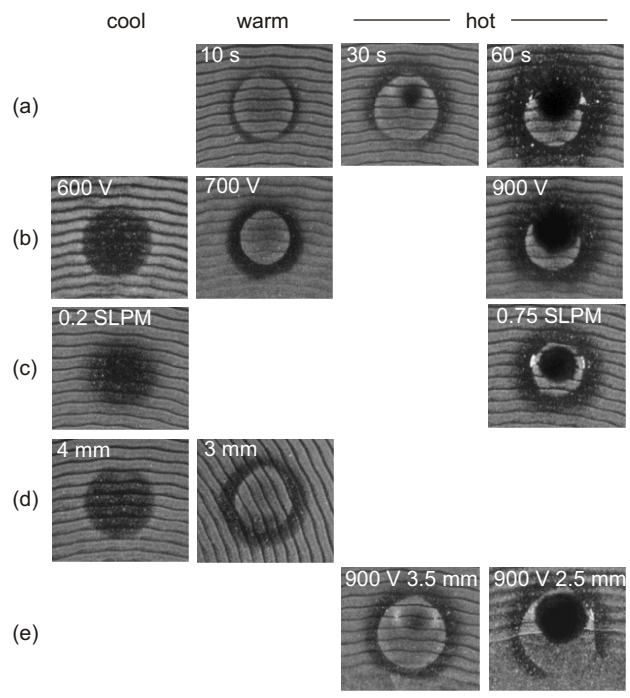


Fig. 4

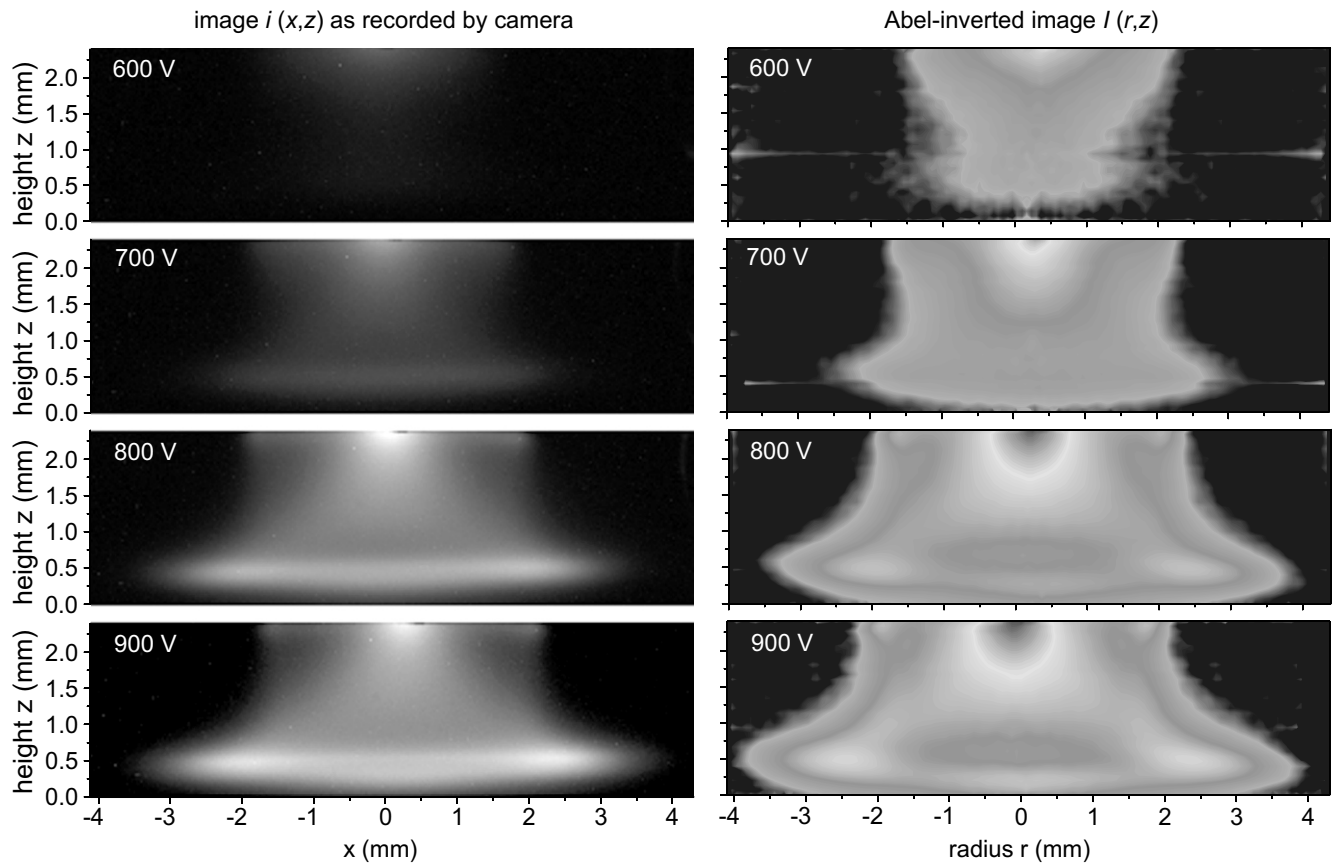


Fig. 5

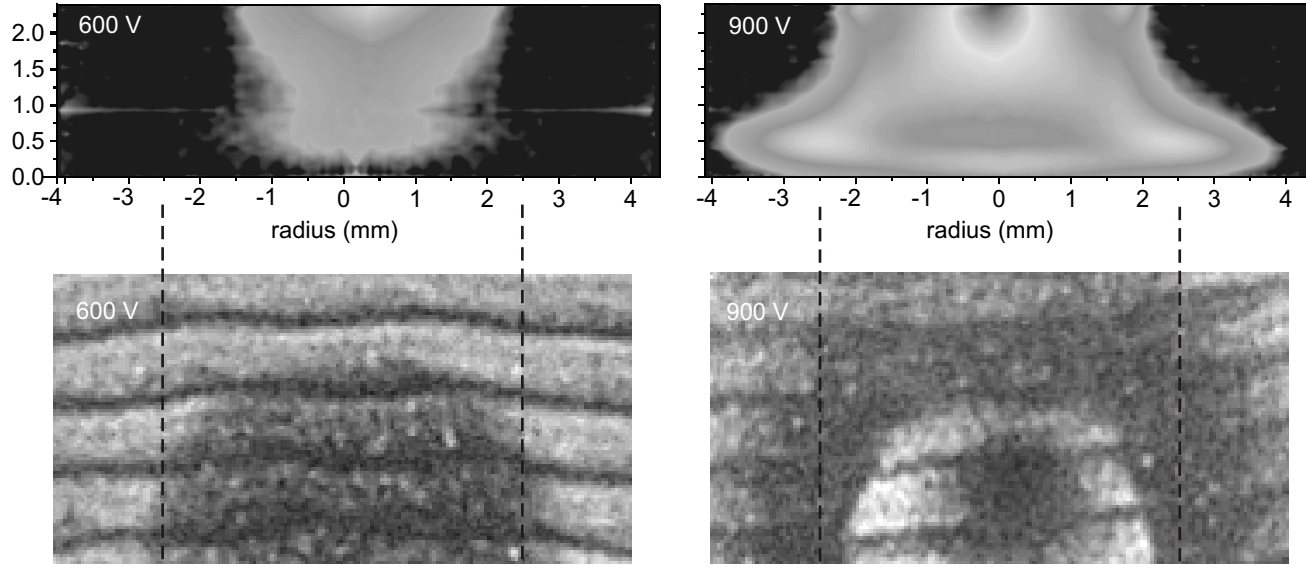


Fig. 6